Article

Decomposition of an odorant in olfactory perception and neural representation

Yuting Ye [1,2,3,9], Yanqing Wang[1,2,4,9], Yuan Zhuang[1,2], Huibang Tan [1,2], Zhentao Zuo [5,6,7], Hanqi Yun[1,2], Kaiqi Yuan [1,2] & Wen Zhou [1,2,8] ✉

Molecules—the elementary units of substances—are commonly considered the units of processing in olfactory perception, giving rise to undifferentiated odour objects invariant to environmental variations. By selectively perturbing the processing of chemical substructures with adaptation ('the psychologist's microelectrode') in a series of psychophysical and neuroimaging experiments (458 participants), we show that two perceptually distinct odorants sharing part of their structural features become significantly less discernible following adaptation to a third odorant containing their non-shared structural features, in manners independent of olfactory intensity, valence, quality or general olfactory adaptation. The effect is accompanied by reorganizations of ensemble activity patterns in the posterior piriform cortex that parallel subjective odour quality changes, in addition to substructure-based neural adaptations in the anterior piriform cortex and amygdala. Central representations of odour quality and the perceptual outcome thus embed submolecular structural information and are malleable by recent olfactory encounters.

Fleeting yet memorable, the smells we experience are triggered by volatile chemical compounds that sorb to the olfactory mucosa and bind to olfactory receptors expressed on the dendrites of olfactory sensory neurons. The olfactory mucosa is considered an analogue of gas chromatography columns, with different odour molecules migrating across it at different rates[1]. The olfactory receptors, over 300 different types in humans[2], have long been theorized to pair with selected odour molecules (primary odorants) in a lock-and-key fashion (shape-pattern theory)[3]. More recent studies indicate that they are broadly tuned to qualitatively distinct compounds and may recognize some general structural determinants for binding rather than the shape of molecules[4,5]. In the olfactory bulb, where the axons of olfactory sensory neurons converge onto stereotypically positioned glomeruli, different odorants evoke distinct and distributed spatial patterns of activity—whether they constitute 'chemotopic maps', mappings of the chemical features of the odorants, is controversial[6–9]. Downstream of the olfactory bulb, the piriform cortex is the main recipient of bulbar afferents and has been shown to represent perceived odour quality, the character of a smell given off by an odorous substance[10–12]. Here odour-induced responses are sparse, diffused and experience-dependent, and individual principal neurons possess discontinuous chemical receptive fields, indicating that they are not tuned to molecular structure[11,13,14]. Despite the reasonable success of predicting olfactory perception from thousands of physicochemical features of odour molecules[15–17], cortical olfactory representations and the perceptual outcomes seem to be synthetic, holistic and memory-bound and do not follow a labelled-line mode[18,19]. Odour compounds are believed to be encoded as undifferentiated wholes that are invariant to variations in stimulus dynamics, history or environmental conditions in central olfactory processing and in perception[10,20–22]. It remains unclear how such unified odour

[1]State Key Laboratory of Brain and Cognitive Science, Institute of Psychology, Chinese Academy of Sciences, Beijing, China. [2]Department of Psychology, University of Chinese Academy of Sciences, Beijing, China. [3]Institute of Psychology, School of Public Affairs, Xiamen University, Xiamen, China. [4]School of Psychology, Northwest Normal University, Lanzhou, China. [5]State Key Laboratory of Brain and Cognitive Science, Institute of Biophysics, Chinese Academy of Sciences, Beijing, China. [6]Institute of Artificial Intelligence, Hefei Comprehensive National Science Center, Hefei, China. [7]Sino-Dannish College, University of Chinese Academy of Sciences, Beijing, China. [8]Chinese Institute for Brain Research, Beijing, China. [9]These authors contributed equally: Yuting Ye, Yanqing Wang. ✉e-mail: zhouw@psych.ac.cn
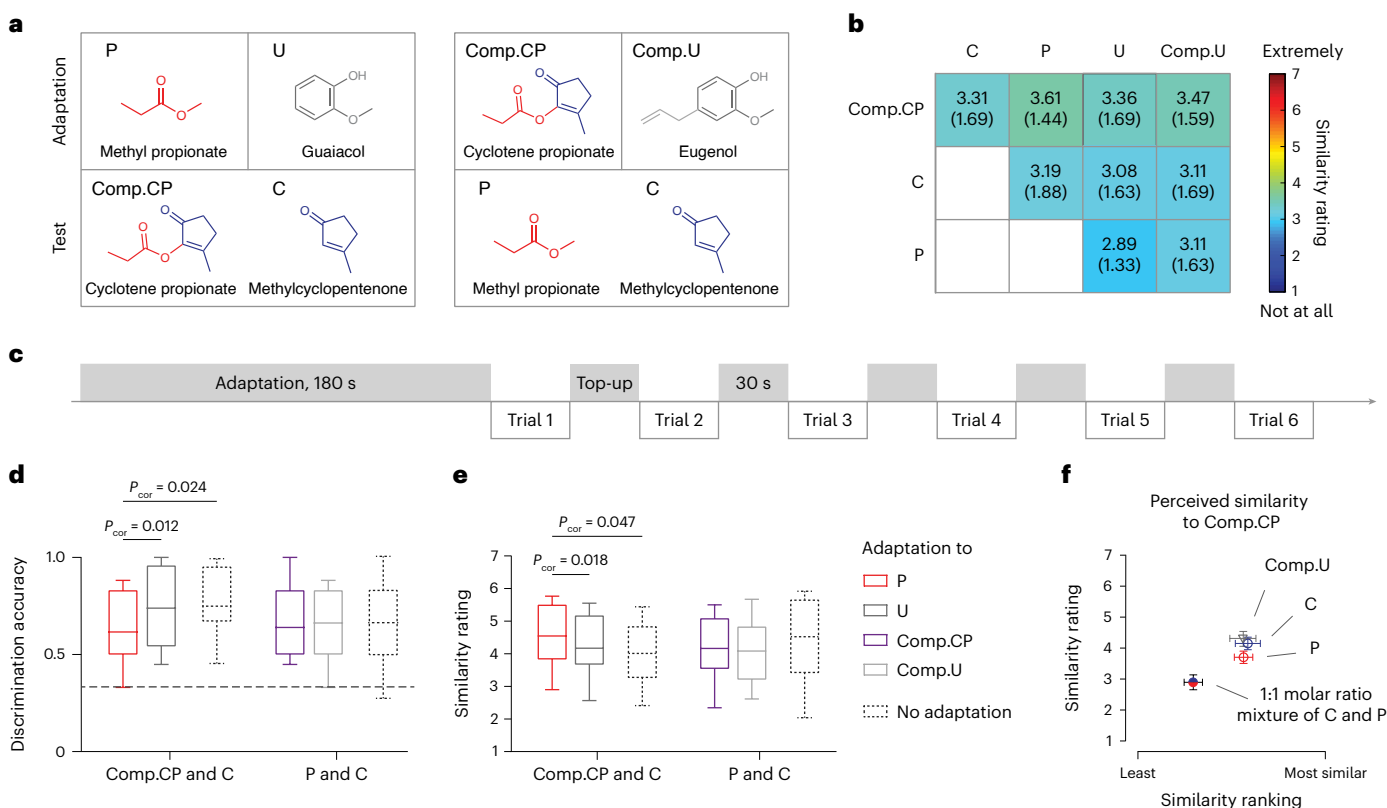
Fig. 1 | Behavioural assessments of substructure−quality relationship. a, The primary olfactory stimuli comprised C, P and Comp.CP. Comp.CP is structurally a composite of C and P. U and Comp.U served as structurally unrelated controls. **b**, Pairwise odour similarity ratings of the olfactory stimuli (mean (s.d.) on a 7-point Likert scale where 7 marked extremely similar; $n = 36$ participants). **c**, Timeline of an experimental session with adaptation. Following a 180 s adaptation to an adapting odour, the participants were assessed for the discrimination and subjective similarity between two other odours in test trials interleaved with 30 s of top-up adaptations. **d,e**, Discrimination accuracies (**d**, triangle test) and subjective similarity ratings (**e**) for Comp.CP and C following adaptations to P and U, respectively, and without adaptation ($n = 36$ each), and for P and C following adaptations to Comp.CP and Comp.U, respectively, and without adaptation ($n = 36$ each). Compared with adaptation to U or no

adaptation, adaptation to P rendered Comp.CP and C less discernible (Δ accuracies, −12.5% and −13.4%; 95% CIs, (−19.7%, −5.1%) and (−23.3%, −3.2%); Wilcoxon $Z = −3.00$ and Mann–Whitney $U = 443$; $P_{cor} = 0.012$ and 0.024; $r_{rb} = 0.59$ and 0.31) and perceptually more similar (Δ similarities, 0.34 and 0.51; 95% CIs, (0.092, 0.59) and (0.0076, 1.01); $t_{35} = 2.78$ and $t_{70} = 2.02$; $P_{cor} = 0.018$ and 0.047; Cohen's $d = 0.46$ and 0.48). In each box-and-whisker plot, the central line, bottom edge and top edge of the box denote the mean, 25th percentile and 75th percentile, respectively. The ends of the whiskers represent the 10th and 90th percentiles. In **d**, the dashed line indicates chance at 0.33. **f**, Perceived similarities of Comp.CP to C, P, Comp.U and a 1:1 molar ratio mixture of C and P in odour quality ($n = 36$). The error bars indicate s.e.m. The P values are false discovery rate (FDR) adjusted for multiple comparisons.

Results

As shown in Fig. 1a, the primary odour compounds we employed were 3-methyl-2-cyclopentenone (C), methyl propionate (P) and cyclotene propionate, whose chemical structure is roughly a composite of C and P (Comp.CP). Two additional compounds served as controls: guaiacol

wholes emerge from chemical compounds entering the nose and to what extent they retain submolecular structural information.

To probe the relationship between submolecular structural features and perceived odour quality, we combined systematic psychophysical assays with functional magnetic resonance imaging (fMRI) and multivariate pattern analysis. We selectively perturbed the processing of certain substructures of an odour compound with adaptation−a mechanism whereby specific neuronal responses decay after repetitive or prolonged stimulation, widely exploited as 'the psychologist's microelectrode'[23]−and examined whether and how it affected the perception and neural representations of that odour compound in human adults. If neural computation of odour quality factors in submolecular information, a breakdown of the holistic odour percept is expected−the percept and its neural representation would be shifted towards those of the unadapted part of that compound. Alternatively, if odour compounds are encoded as invariant wholes, no such shift should occur.

(U), which is structurally unrelated to C, P or Comp.CP; and eugenol (Comp.U)−a composite of U and an allyl group, with a molecular weight close to that of Comp.CP. We quantified pairwise structural similarities among these compounds using the Tanimoto coefficient, which is calculated as the ratio of the number of features common to both molecules to the total number of features, on the basis of common atom pairs and maximum common substructure[24,25]. Both approaches showed higher similarities between Comp.CP and C or P than between any one of them and U or Comp.U (Supplementary Fig. 1a). Nonetheless, such structural relationships did not appear to explicitly manifest themselves in olfactory perception. When matched for perceived intensity ($F_{4,140} = 0.62$, $P = 0.647$), C, P, Comp.CP, U and Comp.U were judged by a panel of 36 participants (17 females; mean age ± s.d., 22.9 ± 0.97 yr) as comparable in valence and familiarity ($F_{4,140} = 0.11$ and 0.13, $P = 0.977$ and 0.973, respectively; Supplementary Fig. 1b) yet dissimilar in quality to one another (<4 on a 7-point scale where 7 marked extremely similar), with no difference in pairwise odour similarity ratings ($F_{5.6,197.2} = 0.78$, $P = 0.579$; Fig. 1b). Another panel of 36 participants (21 females, 22.7 ± 2.39 yr) characterized the odour qualities of C, P, Comp.CP, U and Comp.U using a list of 146 descriptors[26]. Supplementary Table 1 lists the top ten most applicable descriptors for each compound. There was no apparent correspondence between the structural relationships among these compounds and their dominant

odour characters. Pairwise perceptual distances based on the score profiles of the compounds[27] showed that C and P were not perceptually closer to Comp.CP than to Comp.U or than U was to Comp.CP (t_{35} = −0.99 and 1.34, P = 0.330 and 0.189, respectively). The lack of relationship in odour quality was further verified in two independent panels of 36 each. One panel of participants (16 females, 23.6 ± 2.41 yr) was asked to make a forced choice between P and U as to which smelled more similar to each of Comp.CP and C. The other (17 females, 23.0 ± 0.91 yr) was asked to choose between Comp.CP and Comp.U as to which was more similar to each of C and P. The choices were all at chance (binomial test; proportions of choices ≤22/36 versus chance, 0.5; P > 0.121; Supplementary Fig. 1c).

Decomposition of odour quality after substructure adaptation

To critically test for the role of molecular substructure in olfactory perception, we assessed the perceptual similarities between Comp. CP and C after adaptations to P and U, respectively (Fig. 1a, left). Specifically, 36 participants (18 females, 23.2 ± 1.85 yr) were each tested in two sessions held on two consecutive days, with P as the adapting odour in one session and U in the other session (the order was balanced across participants). They judged P and U to be comparable in intensity and valence prior to the test sessions (t_{35} = 1.20 and 0.77, P = 0.238 and 0.444, respectively); so were Comp.CP and C (t_{35} = 1.38 and 0.13, P = 0.176 and 0.899, respectively) (Supplementary Fig. 2a). Each session began with an adaptation phase during which the participants were continuously exposed to the adapting odour for 180 s, followed by six test trials interleaved with 30 s of top-up adaptations (Fig. 1c). In each test trial, they sampled three bottles—either two containing Comp.CP and one containing C or two containing C and one containing Comp.CP—one at a time, and selected the odd one out. They then rated the similarity between the two odours on a 7-point Likert scale, with 7 representing 'extremely similar'. We also recruited a reference group of 36 participants (18 females, 22.4 ± 1.93 yr) who completed the test trials without undergoing adaptation. Our hypothesis was that adaptation to P as opposed to U or no adaptation would make Comp. CP and C smell more alike if the perceptual representation of Comp. CP carries information regarding the structural features of P and C. Analyses of the performances under the three adaptation conditions supported this hypothesis. Following adaptation to P as opposed to U, the participants were significantly poorer at discerning between Comp.CP and C (Δ accuracy, −12.5%; 95% confidence interval (CI), (−19.7%, −5.1%); Wilcoxon Z = −3.00; P = 0.003; P_{cor} = 0.012; rank biserial correlation (r_{rb}), 0.59) and rated them as perceptually more similar (Δ similarity, 0.34; 95% CI, (0.092, 0.59); t_{35} = 2.78; P = 0.009; P_{cor} = 0.018; Cohen's d = 0.46), regardless of the order of the adapting odours (P preceding U versus the reverse: P = 0.300 and 0.460 for discrimination accuracy and similarity rating, respectively) (Supplementary Fig. 2b). Moreover, compared with no adaptation, adaptation to P (which embodied the main structural difference between Comp.CP and C) altered the perceptual similarity between Comp.CP and C (Δ similarity, 0.51; 95% CI, (0.0076, 1.01); t_{70} = 2.02; P = 0.047; P_{cor} = 0.047; Cohen's d = 0.48) and rendered them less discriminable (Δ accuracy, −13.4%; 95% CI, (−23.3%, −3.2%); Mann–Whitney U = 443; P = 0.018; P_{cor} = 0.024; r_{rb} = 0.31), whereas adaptation to the structurally unrelated U exerted no significant impact (t_{70} = 0.64 and Mann–Whitney U = 632, P = 0.527 and 0.853, respectively).

We wondered whether these results were due to general structural relatedness among C, P and Comp.CP or perhaps subtle overlaps in odour subqualities among them[28]. To this end, we further examined the perceptual similarities between C and P after adaptations to Comp. CP and Comp.U as well as without adaptation. Following the same procedures as described above, we recruited and tested two additional groups of 36 participants each. One group (16 females, 22.9 ± 1.92 yr) performed the test trials with C and P after adaptations to Comp.CP and

Comp.U, respectively, in two sessions (Fig. 1a, right). They perceived Comp.CP and Comp.U, as well as C and P, to be comparable in subjective intensity and valence prior to the test sessions (P > 0.060; Supplementary Fig. 2c). The other group of participants (12 females, 22.5 ± 2.25 yr) performed the test trials without undergoing adaptation. The results showed no significant difference in discrimination accuracy (Wilcoxon Z = −0.53, P = 0.595) or similarity rating for C and P (t_{35} = 0.48, P = 0.635) between adaptations to Comp.CP and to Comp.U (Supplementary Fig. 2d). In both cases, the participants' performances were close to those without olfactory adaptation (adaptation to Comp.CP versus no adaptation: Mann–Whitney U = 597 and t_{70} = −1.17, P = 0.559 and 0.247, for discrimination accuracy and similarity rating, respectively; adaptation to Comp.U versus no adaption: Mann–Whitney U = 634 and t_{70} = −1.41, P = 0.876 and 0.163, respectively).

Thus, as summarized in Fig. 1d,e, Comp.CP became perceptually more similar to C after adaptation to P, which essentially represented its difference from C in terms of substructure composition. However, the perceptual similarity of P to C was unaffected by adaptation to Comp.CP, a superstructure of both P and C, presumably because it had symmetric effects on the perceived qualities of P and C. These findings could not be explained by general olfactory adaptation or differences in olfactory intensity, valence or quality among the adaptor and test stimuli. Rather, they pointed to a decomposition of the unified olfactory percept of Comp.CP following substructure adaptation.

Although our data showed no apparent relationship among Comp. CP, C and P in odour quality (Fig. 1b, Supplementary Fig. 1b and Supplementary Table 1), one could argue that Comp.CP might smell like a synergy of C and P[15] and that the observed 'decomposition' simply reflected a more dominant note of C in that mixed percept after one was adapted to the odour of P. To directly address this possibility, we recruited another panel of 36 participants (19 females, 23.2 ± 1.63 yr). In addition to Comp.CP, they were presented with C, P, Comp.U and a 1:1 molar ratio mixture of C and P—all matched in olfactory intensity ($F_{4,140}$ = 0.64, P = 0.632), valence ($F_{4,140}$ = 0.60, P = 0.664) and familiarity ($F_{4,140}$ = 1.61, P = 0.176)—and were asked to rate the similarity of each odour to the odour of Comp.CP and to rank the four odours according to their similarities to Comp.CP. It turned out that the binary mixture of C and P was both rated ($F_{3,105}$ = 8.27, P < 0.001, η_p^2 = 0.19) and ranked (Friedman χ^2_3 = 10.83, P = 0.013) as the least similar to Comp.CP— significantly less similar than C (Δ similarity, −1.33; 95% CI, (−1.99, −0.68); t_{35} = −4.15; P_{cor} < 0.001; Cohen's d = 0.69), P (Δ similarity, −0.86; 95% CI, (−1.51, −0.21); t_{35} = −2.68; P_{cor} = 0.034; Cohen's d = 0.45) or the structurally unrelated Comp.U (Δ similarity, −1.50; 95% CI, (−2.29, −0.71); t_{35} = −3.85; P_{cor} = 0.001; Cohen's d = 0.64) (Fig. 1f).

In two supplementary experiments, we verified that the impact of adaptation to C on the perceptual similarity between Comp.CP and P mirrored that of adaptation to P on the perceptual similarity between Comp. CP and C (Supplementary Experiment 1 and Supplementary Fig. 3). We further replicated the effect of substructure adaptation on perceived odour quality in a new set of odorants—anisole, ethyl acetate and anisyl acetate, whose chemical structure is roughly a composite of anisole and ethyl acetate (Supplementary Experiment 2 and Supplementary Fig. 4). These results demonstrate the generalizability of our findings.

Involvement of primary olfactory processing

Afferent projections from the olfactory epithelium to the olfactory bulb and from the olfactory bulb to primary olfactory regions including the piriform cortex and amygdala are predominantly ipsilateral[29–32]. This allowed us to assess behaviourally, with unilateral adaptation and testing, whether primary olfactory processing critically contributes to the observed alteration of perceived odour quality following substructure adaptation. If this were the case, we predicted that Comp. CP and C would be less discriminable following unilateral adaptation to P relative to U when presented to the adapted nostril but not the unadapted nostril. Unilateral adaptation to P relative to U should also
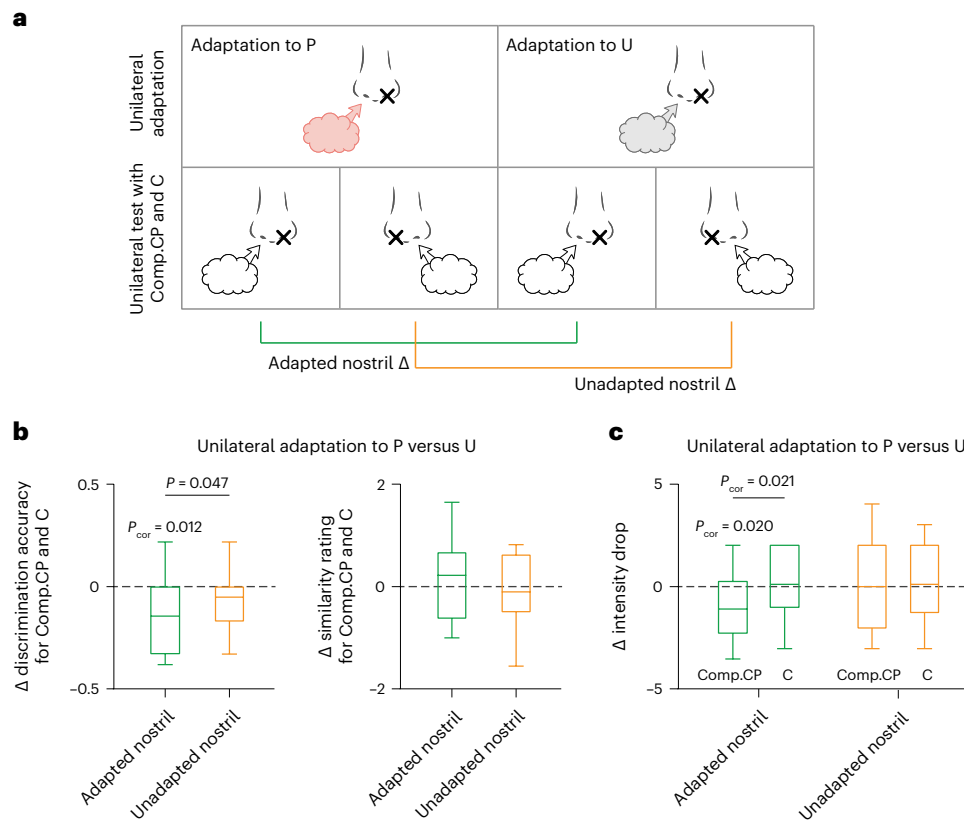
Fig. 2 | Nostril-specific modulation of odour perception by substructure adaptation. a, Participants completed two test sessions where they underwent similar procedures as shown in Fig. 1c, except that the odours were presented unilaterally instead of bilaterally. For each participant, the adapting odours P and U (one for each session) were always presented to a fixed (left or right) nostril. The test odours Comp.CP and C were presented to the adapted nostril in half of the trials of each session and to the unadapted nostril in the other half, in random order. **b**, Differences in odour discrimination accuracy (left) and subjective similarity rating (right) between unilateral adaptations to P and U (post adaptation to P minus post adaptation to U) for Comp.CP and C presented to the adapted nostril and to the unadapted nostril ($n = 36$). Unilateral adaptation to P as opposed to U caused a significant decrease in the discrimination accuracy for Comp.CP and C presented to the adapted nostril (Δ accuracy, −14.4%; 95%

CI, (−21.8%, −6.5%); Wilcoxon $Z = -3.03$; $P_{cor} = 0.012$; $r_{rb} = 0.64$), but not the unadapted nostril, with a significant difference between them (Δ accuracy, −9.2%; 95% CI, (−19.9%, 1.4%); Wilcoxon $Z = -1.99$; $P = 0.047$; $r_{rb} = 0.37$). **c**, Differences in post-adaptation reduction of subjective odour intensity between unilateral adaptations to P and U ((post − pre) adaptation to P − (post − pre) adaptation to U) for Comp.CP and C presented to the adapted and unadapted nostrils ($n = 36$). Within the adapted nostril, adaptation to P relative to U resulted in a significant reduction in the perceived intensity of Comp.CP, and this reduction was more pronounced than that observed for the perceived intensity of C (Δ intensities, −1.08 and −1.19; 95% CIs, (−1.89, −0.28) and (−2.13, −0.26); $t_{35} = -2.74$ and −2.58; $P_{cor} = 0.020$ and 0.021; Cohen's $d = 0.46$ and 0.43). The box-and-whisker plots are as in Fig. 1d,e. The P values are FDR-adjusted for multiple comparisons where applicable.

exert a nostril-specific effect on the perceived intensity of Comp.CP—P's superstructure—rather than C, per the nature of structure-related adaptation[23]. In a similar procedure as described above (Fig. 1c), 36 new participants (18 females, 23.2 ± 1.08 yr) were each tested in two sessions with P as the adapting odour in one session and U in the other (the order was balanced across participants), both presented unilaterally to a fixed nostril (left for 17 participants and right for 19 participants). They rated P and U beforehand to be comparable in odour intensity ($F_{1,35} = 1.30$, $P = 0.263$) regardless of the nostril of presentation ($F_{1,35} = 0.25$ and 0.52, $P = 0.619$ and 0.478 for main effect and interaction, respectively); the same was true of the test odours Comp.CP and C ($F_{1,35} = 0.78$, 0.69 and 0.34; $P = 0.384$, 0.413 and 0.566, respectively) (Supplementary Fig. 5a). The partitioning of nasal airflow, measured by nasal spirometry, was also unbiased between the adapted and unadapted nostrils ($t_{35} = 0.22$, $P = 0.824$) and did not differ between the two sessions ($t_{35} = -1.02$, $P = 0.313$). There were 12 test trials per session: Comp.CP and C were presented to the adapted nostril in six trials and to the unadapted nostril in six trials, in random order (Fig. 2a). Additionally, intensity ratings of the unilaterally presented test odours were collected again at the end of each session. During unilateral odour presentation, the other nostril was always closed by the thumb.

As shown in Fig. 2b, unilateral adaptation to P, compared with the structurally unrelated U, indeed caused a substantial decrease in the participants' discrimination accuracy for Comp.CP and C presented to the adapted nostril (Δ accuracy, −14.4%; 95% CI, (−21.8%, −6.5%); Wilcoxon $Z = -3.03$; $P = 0.002$; $P_{cor} = 0.012$; $r_{rb} = 0.64$), but not the unadapted nostril (Wilcoxon $Z = -1.34$, $P = 0.182$), with a significant difference between them (Δ accuracy, −9.2%; 95% CI, (−19.9%, 1.4%); Wilcoxon $Z = -1.99$; $P = 0.047$; $r_{rb} = 0.37$). The difference in odour similarity ratings of Comp.CP and C across nostrils did not reach statistical significance (adapted versus unadapted nostril: $t_{35} = 1.54$, $P = 0.132$). Moreover, whereas the test odours were generally rated as less intense after adaptation than before adaptation (Δ intensity, −0.77; 95% CI, (−1.30, −0.25); $t_{35} = -2.98$; $P = 0.005$; $P_{cor} = 0.015$; Cohen's $d = 0.50$), the extent of intensity drop showed a significant interaction between the adaptor and the test odours when the latter were presented to the adapted nostril ($F_{1,35} = 6.67$, $P = 0.014$, $P_{cor} = 0.021$, $\eta_p^2 = 0.16$), but not the unadapted nostril ($F_{1,35} = 0.057$, $P = 0.812$). Specifically for the adapted nostril, the perceived intensity of Comp.CP was more influenced by adaptation to its substructure P rather than the structurally unrelated U (Δ intensity, −1.08; 95% CI, (−1.89, −0.28); $t_{35} = -2.74$; $P = 0.010$; $P_{cor} = 0.020$; Cohen's $d = 0.46$; Fig. 2c). By contrast, the intensity of C was not preferentially
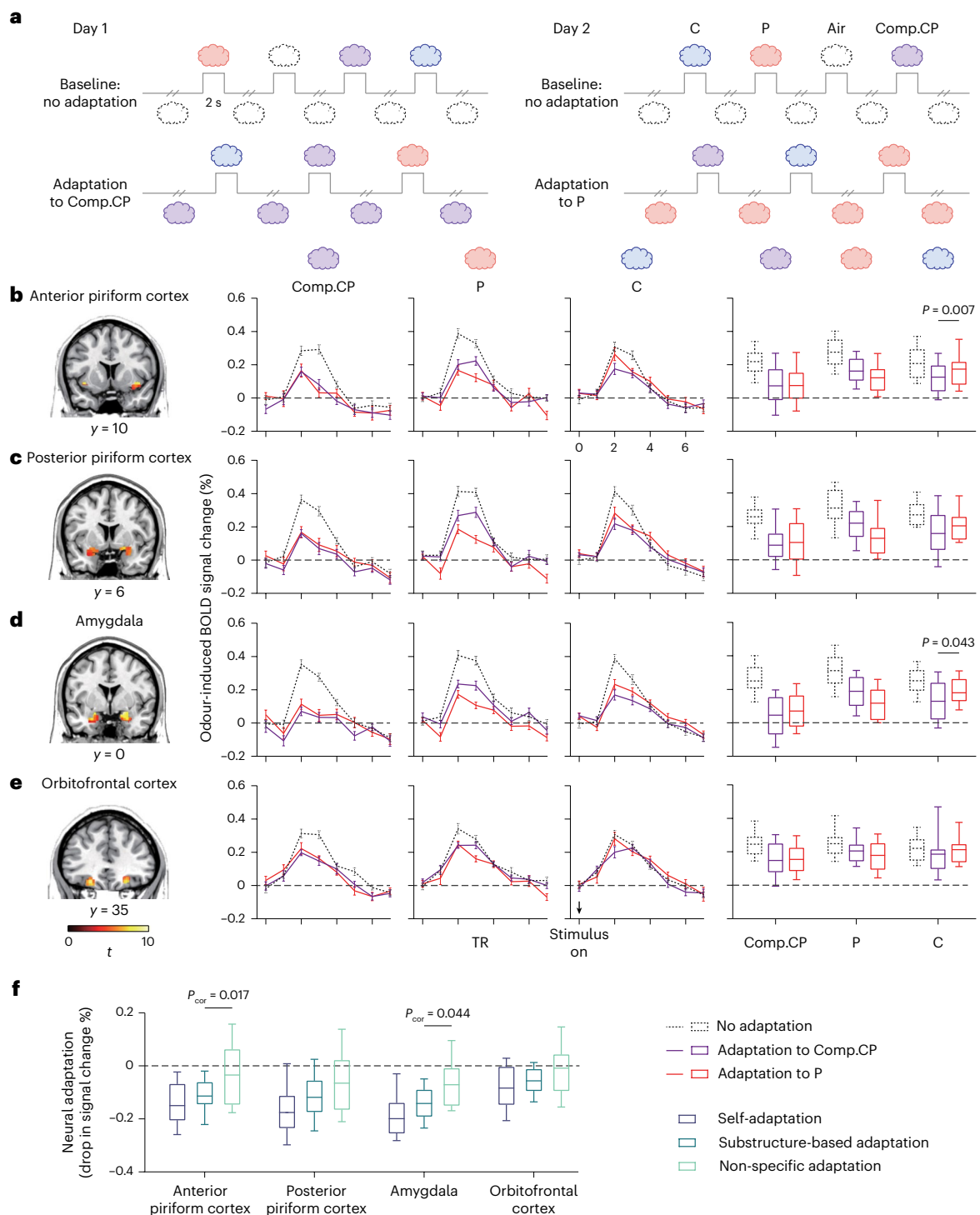
Fig. 3 | Substructure-related neural adaptations. a, fMRI experimental design. The participants were scanned in two sessions on separate days, each comprising two baseline runs without adaptation followed by four adaptation runs where an adapting odour was delivered before the start of the first trial and during all intertrial intervals. **b**–**e**, Group-level activations to odours at the baseline (left, superimposed on coronal sections of the Colin 27 Average Brain) and condition-specific response time courses (middle) and percentage signal changes for the test odours (right) in the anterior piriform cortex (**b**), posterior piriform cortex (**c**), amygdala (**d**) and orbitofrontal cortex (**e**) ($n = 26$). Adaptation to Comp.CP as opposed to P diminished the responses to C in the anterior piriform cortex and the amygdala (Δ percentage signal changes, −0.048 and −0.051; 95% CIs,

(−0.081, −0.014) and (−0.10, −0.0017); $t_{25} = -2.92$ and -2.13; $P = 0.007$ and 0.043; Cohen's $d = 0.57$ and 0.42). The error bars indicate s.e.m. TR, repetition time. **f**, Decrements in odour-induced percentage signal change relative to the baseline following self-adaptation, substructure-based adaptation and non-specific adaptation ($n = 26$). The anterior piriform cortex and the amygdala statistically differentiated between substructure-based adaptation and non-specific adaptation (Δ percentage signal losses, 0.079 and 0.071; 95% CIs, (0.027, 0.13) and (0.018, 0.12); $t_{25} = 3.14$ and 2.75; $P_{cor} = 0.017$ and 0.044; Cohen's $d = 0.62$ and 0.54). The box-and-whisker plots are as in Fig. 1d,e. The P values are Bonferroni-adjusted for multiple comparisons where applicable.

affected by P or U ($t_{35} = 0.34$, $P = 0.733$, $P_{cor} = 0.733$). Notably, the reduction in Comp.CP's subjective intensity following adaptation to P relative to U was unrelated to that in the discrimination accuracy of Comp. CP and C across participants ($r_{36} = 0.11$, $P = 0.540$; Supplementary Fig. 5b), suggesting that the compromised odour discrimination was not a by-product of the decrease in perceived odour intensity. Taken together, these results show that unilateral adaptation to an odour compound modulated the quality and intensity perception of subsequently presented odours in a nostril-specific and substructure-based manner, hence speaking to a key role of the primary olfactory pathway and primary olfactory regions in the change of odour quality following substructure adaptation, and by inference in the synthesis of odour quality from local structural information.

Substructure-based neural adaptations

To clarify the neural correlates of substructure adaptation and the ensuing change in perceived odour quality, we conducted an fMRI experiment and compared blood-oxygen-level-dependent (BOLD) responses to Comp.CP, P and C before and after adaptations to Comp.CP (superstructure of P and C) and P (substructure of Comp.CP) in 26 participants (13 females, 24.0 ± 2.37 yr). Comp.CP, P and C were matched a priori for perceived intensity ($F_{2,50} = 0.55$, $P = 0.581$; Supplementary Fig. 6a). The experiment comprised two scanning sessions held at around the same time of day on two separate days, with Comp.CP as the adapting odour in one session and P in the other session (Fig. 3a). Each session consisted of six runs: two baseline runs without adaptation, followed by four adaptation runs where the adapting odour of that session was delivered (in place of purified air) before the start of the first trial and during all intertrial intervals. On each trial, the participants made a 2 s sniff to air (for the baseline runs), Comp.CP, P or C, presented in a pseudo-randomized order, and indicated whether there was an odour (for the baseline runs) or whether there was an odour different from the background odour (for the adaptation runs). Their hit rates showed an expected effect of adaptation and were significantly lower in the adaptation runs than in the baseline runs (Δ hit rate, −0.13; 95% CI, (−0.17, −0.08); $t_{25} = -5.67$; $P < 0.001$; Cohen's $d = 1.11$). Meanwhile, their sniff patterns (Supplementary Fig. 6b) were stable across all conditions, with no significant effect of test odour or adaptation condition or their interaction in sniff vigour (peak amplitude, $P = 0.726$, 0.918 and 0.557, respectively) or sniff volume ($P = 0.755$, 0.555 and 0.759, respectively).

We analysed fMRI signals in four regions of interest (ROIs) previously implicated in structure and quality coding of odorants as well as subjective olfactory experience: the anterior piriform cortex, posterior piriform cortex and amygdala (key primary olfactory regions) and the orbitofrontal cortex (the main neocortical target of primary olfactory regions)[12,33–36]. The ROIs were defined on the basis of anatomical landmarks and unbiased functional criteria (Methods). All showed robust activations to odours in the baseline runs (Fig. 3b–e, left, and Supplementary Table 2). An omnibus repeated-measures analysis of variance (ANOVA) on odour-induced activities (percentage signal changes) using test odour (Comp.CP, P and C), adaptation condition (baseline, adaptation to Comp.CP and adaptation to P) and ROI as the within-participant factors identified a pronounced effect of adaptation condition ($F_{2,50} = 50.53$, $P < 0.001$, $\eta_p^2 = 0.67$) along with significant interactions between adaptation condition and test odour ($F_{4,100} = 6.08$, $P < 0.001$, $\eta_p^2 = 0.20$) and between adaptation condition and ROI ($F_{4.1,103.1} = 6.19$, $P < 0.001$, $\eta_p^2 = 0.20$), signifying different interplays between test odours and adaptation conditions in different ROIs (Fig. 3b–e, middle and right).

To characterize substructure-related neural adaptation, we calculated the decrement in odour-induced activity from baseline (no adaptation) for each of the combinations of the adaptor and test odours (denoted as Test$_{adaptor}$) and classified them into three categories: self-adaptation (Comp.CP$_{Comp.CP}$ and P$_P$), where the adaptor and test odours were identical in structure and quality; substructure-based

adaptation (Comp.CP$_P$, P$_{Comp.CP}$ and C$_{Comp.CP}$), where they were related in local structural features (sharing the structure of P or C) but dissimilar in quality; and non-specific adaptation (C$_P$), where they were dissimilar in structure and quality. As shown in Fig. 3f, adaptation was overall limited in the orbitofrontal cortex, significantly less than in the anterior piriform cortex, posterior piriform cortex and amygdala ($P_{cor} < 0.039$). Differences among the three types of adaptation were observed in all four ROIs ($P_{cor} < 0.033$), with self-adaptation causing the largest signal drop. Importantly, only the anterior piriform cortex and the amygdala exhibited sensitivity to local features and statistically differentiated between substructure-based adaptation and non-specific adaptation (Δ percentage signal losses, 0.079 and 0.071; 95% CIs, (0.027, 0.13) and (0.018, 0.12); $t_{25} = 3.14$ and 2.75; $P_{cor} = 0.017$ and 0.044; Cohen's $d = 0.62$ and 0.54). To verify this categorical difference between substructure-based adaptation and non-specific adaptation, we performed direct comparisons between C$_{Comp.CP}$ and C$_P$, which eliminated potential confounding factors associated with different test odours. We examined whether the anterior piriform cortex and the amygdala showed reduced activations to C following adaptation to structurally related Comp.CP relative to unrelated P. As expected, adaptation to Comp.CP as opposed to P diminished the responses to C in the anterior piriform cortex (Δ percentage signal change = −0.048; 95% CI, (−0.081, −0.014); $t_{25} = -2.92$; $P = 0.007$; Cohen's $d = 0.57$) and the amygdala (Δ percentage signal change, −0.051; 95% CI, (−0.10, −0.0017); $t_{25} = -2.13$; $P = 0.043$; Cohen's $d = 0.42$) but not in the posterior piriform and orbitofrontal cortices ($P > 0.233$) (Fig. 3b–e, right). These neural adaptation results thus provide evidence that activities in the anterior piriform cortex and amygdala carry local structural information on odour compounds independently of odour quality.

Modification of posterior piriform ensemble pattern

Whereas adaptation is marked by reductions of neural responses and perceptual sensitivity[23], odour quality has been shown to be encoded by the pattern of activity in the posterior piriform cortex[35,37,38]. To examine whether substructure adaptation would alter the ensemble representation of odour quality, we extracted signal values from every odour-responsive posterior piriform voxel and computed the representational similarities between two test odours under different adaptation conditions (Fig. 4a). The underlying hypothesis was that adaptation to P would render the posterior piriform representations for Comp.CP and C more alike, yet adaptation to Comp.CP would not influence the representational similarity between C and P. Consistent with this hypothesis, we found that compared with the baseline, the spatial pattens for Comp.CP and C became significantly more correlated following adaptation to P (Fisher Z-transformed r, Δ = 0.16; 95% CI, (0.066, 0.24); $t_{25} = 3.58$; $P = 0.001$; Cohen's $d = 0.70$). Those for C and P were no more or less correlated following adaptation to Comp. CP ($t_{25} = 0.21$, $P = 0.838$) (Fig. 4b). These results dovetail with the earlier observations that adaptation to P made Comp.CP and C perceptually more similar and less discernible, and that adaptation to Comp.CP had no impact on the perceptual similarity between C and P (Fig. 1d,e). Additional exploratory analyses indicated that the parallel between correlations of neural activity patterns and behavioural discriminations or judgements of odours was specific to the posterior piriform cortex. The spatial correlations for Comp.CP and C and for C and P in the anterior piriform cortex, amygdala and orbitofrontal cortex stayed unchanged before and after adaptations to P and Comp.CP ($P > 0.250$, Fig. 4b).

Odour maps for each test odour and adaptation condition from one exemplar participant (Fig. 4c) illustrate how spatial patterns of activity in the posterior piriform cortex varied across conditions. On top of significant reductions in the magnitude of mean activation following adaptation (see also Fig. 3c,f), a reorganization of the activity pattern for Comp.CP from the baseline to post-adaptation to P was particularly evident. Difference maps further show that the spatial patterns for Comp.CP and C converged following adaptation to P that essentially
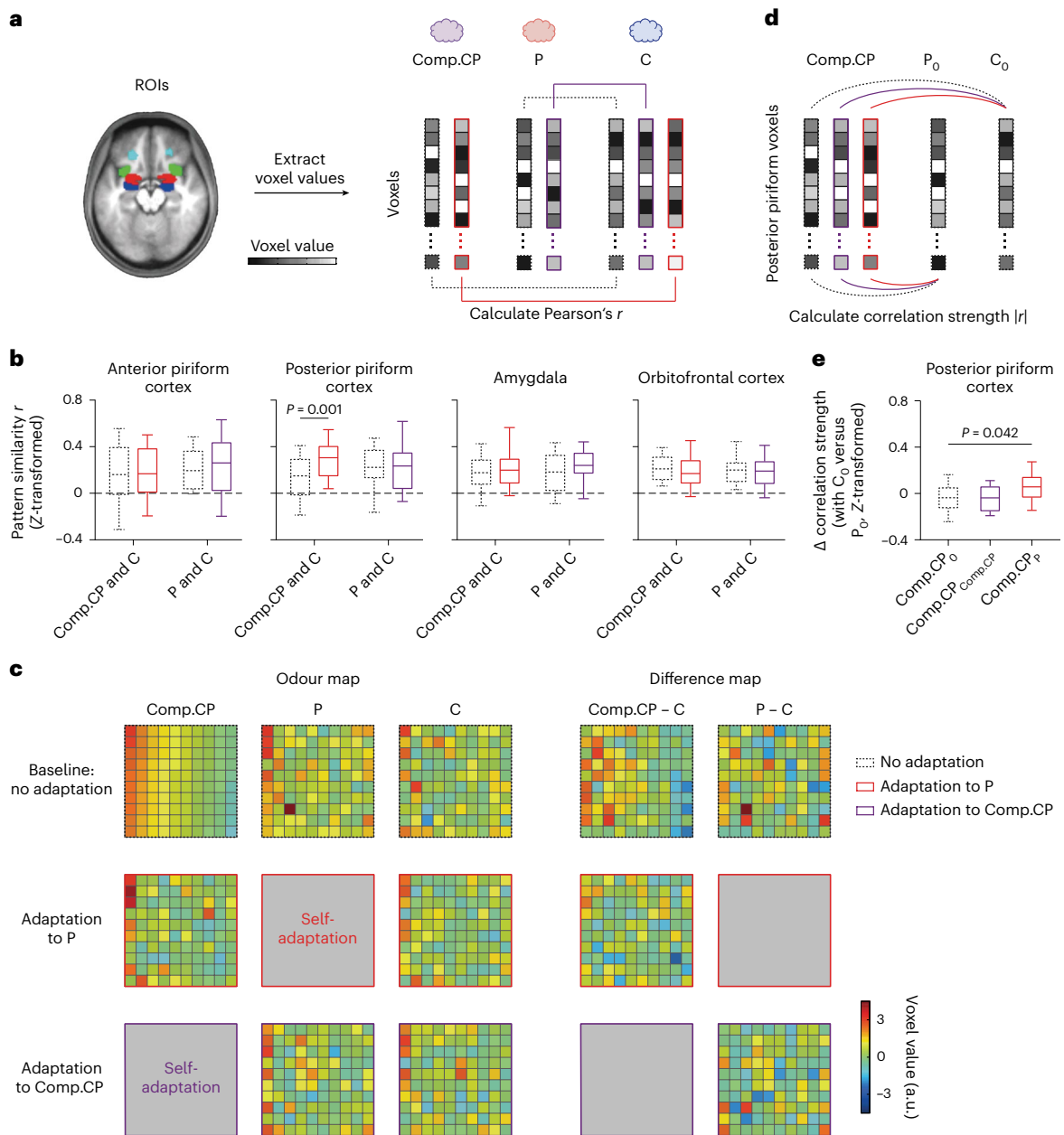
Fig. 4 | Selective reorganization of posterior piriform activity pattern following substructure adaptation. a, Representational similarity between two test odours in an ROI was computed as the Pearson correlation across voxels within that region. **b**, Representational similarities for Comp.CP and C at the baseline and following adaptation to P and for P and C at the baseline and following adaptation to Comp.CP in the anterior piriform cortex, posterior piriform cortex, amygdala and orbitofrontal cortex ($n = 26$). The representations of Comp.CP and C in the posterior pirifrom cortex became more correlated following adaptation to P, compared with the baseline (Fisher Z-transformed r, $\Delta = 0.16$; 95% CI, (0.066, 0.24); $t_{25} = 3.58$; $P = 0.001$; Cohen's $d = 0.70$). **c**, Spatial maps of odour-induced posterior piriform activity patterns (left) and pattern differences (right) from an exemplar participant. The cells represent signal values from voxels within the posterior piriform cortex ROI, arranged in descending order of signal value for Comp.CP at the baseline. **d**, The relative representational proximity of Comp.CP to its two substructures under each adaptation condition was computed as the difference between the correlation strengths of Comp.CP to C_0 and P_0 in terms of voxel-wise activity patterns in the posterior piriform cortex ($|r_z(\text{Comp.CP}, C_0)| - |r_z(\text{Comp.CP}, P_0)|$). **e**, Relative representational proximities of Comp.CP to C_0 against P_0 at the baseline and following adaptations to Comp.CP and P, respectively, in the posterior piriform cortex ($n = 26$). The activity pattern for Comp.CP changed towards that for C_0 and away from that for P_0 following adaption to P, compared with the baseline ($\Delta = 0.095$; 95% CI, (0.0039, 0.19); $t_{25} = 2.15$; $P = 0.042$; Cohen's $d = 0.42$). The box-and-whisker plots are as in Fig. 1d,e.

embodied the structural difference between the two compounds. In contrast, those for C and P remained distinct following adaptation to Comp.CP—their superstructure—despite the aforementioned substructure-based adaptation in the strengths of neural responses.

The post-adaptation pattern changes described above clearly demonstrate a spontaneous reorganization of posterior piriform activity patterns following adaptation. They also imply that the reorganization was not random but informed by the structural relationship between the adaptor and test odours. To probe the underlying computational principles, we calculated the correlation strengths of the spatial patterns for Comp.CP under different adaptation conditions to those for C and P at the baseline (that is, C_0 and P_0; the subscript '0' refers to the baseline; Fig. 4d). We then quantified, for each of Comp. CP_0, Comp.CP$_{\text{Comp.CP}}$ and Comp.CP$_P$, the extent to which the ensemble

representation was more akin to the original pattern of C than that of P—that is, the relative proximity of Comp.CP to its two separate substructures in terms of representational distance[39]. In other words, we tested whether adaptation to P would particularly shift the representation of Comp.CP towards that of C_0 rather than P_0. The results (Fig. 4e) show that, compared with the baseline, the activity pattern for Comp. CP significantly changed towards that for C_0 and away from that for P_0 following adaption to P (Comp.CP_P versus Comp.CP_0: $\Delta = 0.095$; 95% CI, (0.0039, 0.19); $t_{25} = 2.15$; $P = 0.042$; Cohen's $d = 0.42$), but not to Comp. CP (Comp.$CP_{Comp.CP}$ versus Comp.CP_0: $t_{25} = -0.015$, $P = 0.988$). The difference between adaptations to P and Comp.CP was also numerically evident but did not reach statistical significance (Comp.CP_P versus Comp.$CP_{Comp.CP}$: $\Delta = 0.095$; 95% CI, (−0.0071, 0.20); $t_{25} = 1.92$; $P = 0.067$; Cohen's $d = 0.38$). Hence, substructure adaptation seems to selectively modify the ensemble representation of odour quality in the posterior piriform cortex, rendering it more similar to the pattern for the unadapted, as opposed to the adapted, part of an odorant.

Discussion

A molecule is the fundamental unit of a compound that retains its physical and chemical properties. An odorant molecule is commonly considered the unit of processing in olfactory perception, whose shape or intramolecular vibrations are believed to be recognized and holistically interpreted as a particular smell[3,40,41]. Here we present compelling behavioural and neuroimaging data that convergently demonstrate a sensitivity to submolecular structural features in human olfactory perception: adaptation to a substructure of an odour compound resulted in a significant alteration of the perceived quality of that compound, paralleled by reductions of neural responses in the anterior piriform cortex and the amygdala as well as a reorganization of the ensemble activity pattern in the posterior piriform cortex that manifested the two odorants' structural relationship. These findings establish a direct correspondence between the coding of local chemical structure and that of olfactory quality, which has been elusive in previous studies[42], and unveil an atomistic (analytical) component of olfactory perceptual processing whereby odour quality is computed on the basis of atomistic parts (submolecular features) and compositional rules[43]. Moreover, these results argue against an invariant perceptual or neural representation of an odorant's quality or identity. Rather, the representations can be dynamically modified by recent olfactory experience, in reference to the structural relationship of the preceding stimulus to the current one.

Our findings appear to be connected with, albeit different from, the phenomenon of cross adaptation—the decrease in sensitivity to one odorant following adaptation to a different odorant[44,45]. Cross adaptation takes place between structurally or perceptually similar compounds[46–48]. It has long been theorized to reflect the extent to which different odours share coding channels, hence providing a basis for odour classification, and has been utilized to delineate representations of functional group and quality in the human piriform cortex[33,44,46–48]. Here, in addition to a reduction in perceived intensity (sensitivity), substructure adaptation further produced a significant change in perceived quality towards that of the unadapted part of an odorant; the effect was obtained in spite of the modest configural similarity and the lack of qualitative similarity between the adaptor (substructure) and test odorants (Fig. 1a,b and Supplementary Figs. 1 and 4a–d). This 'decomposition' of odour quality, previously unsuspected, sheds new light on the neural computation underlying the formation of a smell or an odour object and could provide a novel strategy for malodour management. However, it does not necessarily represent a failure of olfactory perceptual constancy[10], as constancy requires experience[49] yet the odour compounds used in the current study were generally perceived as not familiar.

The short-term effect of substructure adaptation is behaviourally and mechanistically different from the relatively long-term effect of odour habituation[50,51]. Prolonged exposure to an odorant has been demonstrated to decrease perceptual similarity between the habituated odorant and a quality-related or functional-group-related odorant in a manner that involves spontaneous recovery of the habituated response[52]. The current study did not use the adapted odorant itself in the odour discrimination/similarity rating tasks. Decreased discrimination or increased similarity was observed between two test odorants whose non-shared structural features were contained in the adapted odorant immediately following adaptation. In essence, substructure adaptation is used here as a probe to dissect the representation of an odorant and does not entail long-term neural plasticity.

On the surface, the computation of the olfactory quality of a monomolecular odorant from submolecular structural features may seem equivalent to that of an odorant mixture from the structures of monomolecular components[15]. This simplified view is contradicted by our observation that a 1:1 molar ratio mixture of two monomolecules C and P smells distinctively different from their structural composite Comp.CP, more so than C, P and structurally unrelated Comp.U. The perceptual dissimilarity between Comp.CP and the binary mixture of C and P denotes different interactions of intramolecular bonds and intermolecular forces with the olfactory system (for example, mucosal sorption and receptor binding affinity). Exactly how they are factored in the neural computation of odour quality awaits future research.

The neuroimaging results resonate with the known functional anatomy of the olfactory system. Much of this knowledge comes from anatomical and neurophysiological studies in non-human animals. Human neuroimaging studies have also demonstrated the different functional roles of the anterior and posterior piriform cortices. The anterior piriform cortex receives mostly feed-forward input from the olfactory bulb—where stereotypically positioned glomeruli are tuned to specific molecular features[8,53]—and has been suggested to encode odorant structure irrespective of odour quality[14,33,54]. Bulbar projections to the cortical amygdala are also spatially stereotyped[36], which could confer the latter an anatomical context for the extraction and comparison of structural information. The posterior piriform cortex, by contrast, receives mostly associational inputs from nearby regions[14]. Separate lines of evidence indicate that it transforms the chemical feature space inherited from the bulb into a space that corresponds more to perceived odour quality[11,35,37,54]. These regions also send feedback projections back to the olfactory bulb to form recurrent loops[12]. Nonetheless, our data from the unilateral adaptation and test experiment, along with other animal studies in the field[55–57], indicate a critical role of exposure-dependent bottom-up processing in the synthesis of odour quality. Given the link between adaptation and sparse representation by which the piriform cortex is characterized[14,58], it is conceivable that the reorganization of the posterior piriform activity pattern following substructure adaptation is mediated by adapted input from the anterior piriform cortex and amygdala that coveys local structural information of an odour compound. Due to magnetic susceptibility differences from air/tissue interfaces, no reliable BOLD signal is detected in the olfactory bulb or olfactory epithelium. Nonetheless, substructure adaptation probably originates in these upstream regions known to be sensitive to molecular features[4,5,8,53]. Put differently, the effect of adaptation to local chemical structural features cascades to downstream regions (as has been demonstrated in vision[59]) and alters the perceptual outcome. Adaptation is ubiquitous in olfaction and takes place within a sniff bout[60]. In this light, and on the basis of computational studies that relate olfactory percepts to the molecular structures of odorants[15–17,61], we propose that the smells we perceive are the products of continuous analysis and synthesis in the olfactory system, breath by breath, of the structural features and relationships of volatile compounds in our ever-changing chemical environment.

Methods

The study was conducted in accordance with the ethical standards set forth in the Declaration of Helsinki and was approved by the

Institutional Review Board at the Institute of Psychology, Chinese Academy of Sciences (H18029).

Participants

A total of 458 healthy non-smokers with no history of neurological disorders participated in the study. Of these, 386 participated in the main study and 36 in each of Supplementary Experiments 1 and 2. For the main study, 360 participants took part in the various behavioural assessments (36 participants per condition or task), and 26 participated in the fMRI experiment. All participants reported having a normal sense of smell and no respiratory allergy or upper respiratory infection at the time of testing. Those who took part in the unilateral adaptation and test also had no significant nasal septal deviation as measured by nasal spirometry, with nasal partitioning ratios ranging between −0.3 and 0.3 (ref. 62). The participants were not informed about the relationships among the olfactory stimuli or the purposes of the experiments. Upon completion of the experiment, they received monetary compensation for their time: 50 RMB per hour for behavioural assessments and 100 RMB per hour for neuroimaging. Written informed consent and consent to publish were obtained from all participants. Regarding sample sizes, we were unaware of any previous study on substructure adaptation and odour quality change and thus could not perform a formal power analysis. The sample size in each experiment (or cell) was about twice the size used in previous studies on related topics[33–35,38,46–48].

Olfactory stimuli and delivery

As shown in Fig. 1a, the primary olfactory stimuli consisted of C (CAS no. 2758-18-1, Shanghai Acmec Biochemical), P (CAS no. 554-12-1, Sigma-Aldrich) and Comp.CP (CAS no. 87-55-8, Shanghai Acmec Biochemical). C and P are both substructures of Comp.CP. Two additional compounds, U (CAS no. 90-05-1, Sigma-Aldrich) and Comp.U (CAS no. 97-53-0, Sigma-Aldrich), served as structurally unrelated controls in the behavioural assessments. Comp.U is a composite of U and an allyl group and has a molecular weight close to that of Comp.CP. Supplementary Table 3 summarizes the olfactory stimuli employed in each experiment of the main study and their respective liquid-phase concentrations. Propylene glycol (CAS no. 57-55-6, Sigma-Aldrich) was used as the solvent. The olfactory stimuli employed in Supplementary Experiments 1 and 2 are described in the Supplementary Information. All olfactory stimuli were presented at room temperature and were supra-threshold to the participants. Note that in the behavioural adaptation experiments, higher concentrations were used for the adaptor stimuli to maximize the effect of adaptation.

The olfactory stimuli in the behavioural assessments were presented in identical 280 ml narrow-mouthed glass bottles, coded by an individual not involved in the assessments. Each bottle contained 10 ml of clear liquid and was fitted with one (for the unilateral adaptation and test) or two (for all other behavioural experiments) Teflon nosepieces. The participants were instructed to inhale through the nosepieces and exhale through the mouth when sampling the olfactory stimuli. The olfactory stimuli in the fMRI experiment were presented using an MRI-compatible computer-controlled olfactometer (Emerging Tech Trans) at a flow rate of 3.5 l min⁻¹.

Behavioural assessments

Odour evaluations of single compounds. A panel of 36 participants sampled C, P, Comp.CP, U and Comp.U one at a time in random order, and provided ratings of the intensity, valence and familiarity of each compound on 7-point Likert scales, where 7 marked extremely intense, pleasant and familiar, and 1 marked not at all intense, pleasant and familiar, respectively. They were then presented with nine odour pairs, Comp.CP–C, Comp.CP–P, Comp.CP–U, Comp.CP–Comp.U, C–P, C–U, C–Comp.U, P–U and P–Comp.U, one pair at a time in random order, and were asked to rate the perceptual similarity (in terms of odour quality) between the two odours in each pair on a 7-point Likert scale, with 7

representing extremely similar and 1 representing not at all similar. The relationships in odour quality among these compounds were further examined using a two-alternative forced-choice task in two additional panels of 36 participants each. In each trial, the participants sampled three odours, a target and two choices, and picked from the two choices the one that smelled more like the target. Comp.CP and C served as the target stimuli, and P and U served as the choice stimuli for one panel of participants; C and P served as the target stimuli and Comp.CP and Comp.U the choice stimuli for the other panel. There was a break of at least 30 s between two trials to eliminate olfactory adaptation. The rating scales and procedures were employed in subsequent experiments where applicable.

Odour character profiles. A panel of 36 participants characterized the odour qualities of C, P, Comp.CP, U and Comp.U using a list of 146 descriptors[26]. For each compound, they scored the suitability of each descriptor to its odour on a scale of 0 to 5. They were allowed to resample the odour as needed in this process. The percentage applicability of each descriptor to each compound was calculated on the basis of the percentage of participants who used that descriptor for that compound and the sum of scores for the panel[26]. Moreover, pairwise perceptual distances were quantified on the basis of the score profiles of the compounds[27].

Odour similarities under different adaptation conditions. A total of 144 participants were randomly assigned to four groups of 36 each: two adaptation groups (Groups 1 and 3) and two reference groups (Groups 2 and 4). Those in Group 1 first provided intensity and valence ratings for P, U, Comp.CP and C (Fig. 1a, left) and were then tested in two sessions held at the same time of day on two consecutive days, with P and U as the adapting odours, respectively (the order was balanced across the participants). Each session comprised a 180 s adaptation phase followed by six test trials interleaved with 30 s of top-up adaptations (Fig. 1c). In each test trial, the participants, blindfolded, were presented with three bottles—either two containing Comp.CP and one containing C (three trials) or two containing C and one containing Comp.CP (three trials)—one at a time in random order, and were asked to pick the odd one out (chance = 0.33) and then to rate the similarity between the two odours they had just smelled. During the adaptation phases, they continuously inhaled through the bottle containing the adapting odour of that session and exhaled through the mouth. Those in Group 2 were tested in a single session where they performed the test trials with Comp.CP and C without adaptation. There was instead a 30 s break between two test trials. Groups 3 and 4 underwent the same procedures as Groups 1 and 2, respectively, except that different odour compounds were employed (Fig. 1a, right): Comp.CP and Comp.U served as the adapting odours for Group 3; P and C served as the test odours for both Groups 3 and 4.

Odour similarity between Comp.CP and a mixture of C and P. A panel of 36 participants provided intensity, valence and familiarity ratings for each of Comp.CP, C, P, Comp.U and a 1:1 molar ratio mixture of C and P (C + P) and rated the perceptual similarities between Comp.CP and each of the other four odours. They also performed a ranking task where they freely sampled the five odours and ranked C, P, Comp.U and C + P on the basis of their perceptual similarities to Comp.CP. There was a break of at least 30 s between two trials.

Unilateral adaptation and test. A group of 36 participants underwent similar procedures as Group 1 described above, but the odours were presented unilaterally (to a single nostril) instead of bilaterally (to both nostrils). Specifically, the adapting odours P and U were always presented to a fixed nostril in the test sessions (Fig. 2a): left for 17 and right for 19 participants. After the initial 180 s adaptation phase of each session, the participants completed 12 unilateral test trials interleaved with 30 s of top-up adaptations. The test odours Comp.CP and

C were presented to the left nostril in six trials and to the right nostril in the other six trials, in random order. Intensity ratings of unilaterally presented Comp.CP and C were collected again after the completion of the test trials. Additionally, the partitioning of airflow between the adapted and unadapted nostrils was assessed with a rhinospirometer (GM Instruments) at the beginning and end of each session. During unilateral odour presentations, the unexposed nostril was always closed by the thumb.

Unless otherwise specified (for example, adaptation phase and free sampling), each odour was presented for about 2 s in a trial in the behavioural assessments.

Behavioural analysis. Odour discrimination accuracies were not normally distributed (Shapiro–Wilk test of normality, $P \leq 0.021$ for all groups and conditions) and were analysed with non-parametric tests: the Wilcoxon signed-rank test for within-group comparisons and the Mann–Whitney test for between-group comparisons. We provide 95% bootstrap confidence intervals. The effect size was estimated using r_{rb}. Comparisons of odour ratings within and between groups were performed using the paired-samples t-test, repeated-measures ANOVA and independent-samples t-test. The effect size for t-tests was estimated using Cohen's d; that for ANOVAs was estimated using η_p^2. In addition, responses in the two-alternative forced-choice odour similarity task were analysed with the binomial test. Ranks of odours in the odour similarity ranking task were compared using the Friedman test. All statistical tests were two-tailed, where applicable. Post hoc tests were Bonferroni corrected. Given that multiple planned comparisons were conducted to evaluate the effects of substructure adaptation, and the test statistics (for example, discrimination accuracy and subjective odour similarity) were positively correlated, we applied FDR corrections to all substructure-adaptation-related tests within each experiment and reported the corrected P values (Supplementary Information and Supplementary Table 4). Notably, we also applied FDR corrections across all substructure-adaptation-related tests in all experiments. In both cases, all originally significant tests survived the corrections at $q = 0.05$.

fMRI experiment

Procedure. Twenty-six right-handed participants took part in the fMRI experiment, which employed a full within-participant design and comprised two scanning sessions held at around the same time of day on two separate days. There were six runs of approximately 6 min each per session: two baseline runs without adaptation followed by four adaptation runs with Comp.CP as the adapting odour in one session and P in the other session (Fig. 3a). Throughout each run, inhalations (2 s) and exhalations (2 s) were prompted by words on the screen so that breathing could be synchronized with odour delivery. The breathing prompts were mostly presented in white; their colour changes served as attentional prompts (yellow) and sniff cues (green). In the baseline runs, each trial began with a 2 s attentional prompt (the word 'exhale' presented in yellow), after which the participants were cued to take a 2 s sniff (the word 'inhale' presented in green). They then pressed one of two buttons to indicate whether there was an odour. There were 14 trials per run: Comp.CP, P, C and purified air were each presented during the sniff cue in four, four, four and two trials, respectively, in a pseudo-randomized order. The interstimulus interval was jittered between 18 and 30 s, during which purified air was continuously delivered. In the adaptation runs, an adapting odour was presented before the onset of the first test odour and during all interstimulus intervals, which ranged between 18 and 26 s. Each run consisted of 13 trials: Comp.CP, P and C were each presented in three, five and five trials, respectively, when Comp.CP was the adapting odour, and in five, three and five trials, respectively, when P was the adapting odour. The task was to indicate whether there was an odour different from the background odour. The procedure was otherwise identical to that in

the baseline runs. Respiration was monitored with a pneumogram sensor (RX110-MRI) taped on the diaphragm and recorded using Biopac MP150 (Biopac Systems). Stimulus presentation, response registration and their synchronization with respiration recording (via a parallel port) and MR image acquisition (trigger pulses from the scanner) were controlled using E-Prime 2 (Psychology Software Tools).

Imaging parameters. Imaging data were collected with a Siemens 3T Prisma Fit scanner and a 20-channel head coil. Gradient-echo T2*-weighted echoplanar images (EPI) were acquired with two sets of parameters due to a major software update. For 17 participants, TR, 2 s; echo time, 27 ms; flip angle, 90°; matrix, 96 × 96; field of view, 192 × 192 mm²; in-plane resolution, 2.0 × 2.0 mm²; slice thickness, 2 mm; gap, 0; number of slices, 34; and acquisition angle, 30° rostral to the intercommissural line. For 9 participants, a blipped-controlled-aliasing multiband EPI sequence was employed; TR, 2 s; echo time, 29 ms; flip angle, 80°; matrix, 128 × 128; field of view, 192 × 192 mm²; in-plane resolution, 1.5 × 1.5 mm²; slice thickness, 1.5 mm; gap, 0; number of slices, 88; and acquisition angle, 0° to the intercommissural line. A 1 mm³ isotropic T1-weighted anatomical volume, along with a field map, was also acquired for each participant. Note that all fMRI results were based on within-participant comparisons, which accounted for interindividual differences due to imaging parameters or other extraneous factors. Moreover, no difference was found between the two subsets of participants scanned with different sets of imaging parameters in any of the measures examined ($P > 0.075$).

fMRI preprocessing. Functional data were preprocessed with SPM v.12 (http://www.fil.ion.ucl.ac.uk/spm). EPI images were corrected for slice timing differences and geometric distortion due to susceptibility artefacts (using the participants' field maps) and were spatially realigned to the first volume of the first session (the first baseline run on Day 1) and unwarped to reduce movement-related variance. For the univariate analysis, this was followed by spatial smoothing (6 mm full width at half maximum (FWHM) Gaussian kernel) to enhance the signal-to-noise ratio and temporal filtering (128 s high-pass filter) to eliminate low-frequency drifts. Spatial normalization was not performed except for the purpose of displaying group-level odour-induced activations at the baseline (Fig. 3b–e, left, and Supplementary Table 2), in which case the images from the baseline runs were spatially normalized to a standard EPI template (MNI space, 2 mm isotropic resolution) and then spatially smoothed and temporally filtered before further analysis. For representational similarity analysis, no additional preprocessing was performed to preserve the spatial fidelity of the signals.

Definition of ROIs. The anterior piriform cortex and the posterior piriform cortex were manually drawn on each participant's anatomical scan, coregistered to his or her mean realigned EPI image, according to an anatomical atlas[63]. The location where the basal frontal lobe first joins the medial temporal lobe in the coronal T1 sections served as the landmark to delineate the caudal extent of the anterior piriform cortex and the rostral extent of the posterior piriform cortex[38]. The amygdala was defined using cytoarchitectonic probabilistic maps integrated in the SPM Anatomy toolbox[64]. The olfactory orbitofrontal cortex was defined on the basis of a meta-analysis of human neuroimaging studies on olfactory processing[65], drawn as 6-mm-radius spheres centred on MNI coordinates (−22, 32, −18) and (24, 33, −12). These structural masks were projected into each participant's native EPI space and functionally restricted to voxels that responded to odours at the baseline (in the baseline runs, $P < 0.01$)[38]. The functionally restricted ROIs were employed in subsequent analysis.

Univariate analysis. Our slow event-related design enabled us to characterize the haemodynamic response triggered by each test odour (Comp.CP, P and C) under each adaptation condition (baseline,

adaptation to Comp.CP and adaptation to P) in a voxel-wise manner. Specifically, the 3 × 3 combinations of test odours and adaptation conditions were modelled with a set of impulse response functions from 0 to 16 s post stimulus (eight time bins of 2 s each, TR 0 to TR 7) that made no assumption about the shape of the response. Head motion parameters were included as nuisance regressors, and serial autocorrelations were modelled as an autoregressive process. The signal changes over TRs were then extracted per ROI and per participant (in the native EPI space) with MarsBaR (https://marsbar-toolbox.github.io/) (Fig. 3b–e, middle). The mean values for TR 2, TR 3 and TR 4 (peak time points) indexed odour-evoked percentage signal changes (Fig. 3b–e, right) and were subsequently analysed with repeated-measures ANOVAs and paired-samples t-tests. Multiple comparisons across ROIs and conditions were Bonferroni corrected where applicable.

Multivariate representational similarity analysis. Effects of no interest (motion regressors and low-frequency drift) were first subtracted out from the preprocessed functional data with AFNI programs 3dDeconvolve and 3dSynthesize (https://afni.nimh.nih.gov/). Values from post-stimulus TR 3, the time point that best captured signal variations across conditions, were then extracted from the voxels within each ROI (in the native EPI space) for each of the combinations of test odours and adaptation conditions, which formed the input to representational similarity analysis. For each adaptation condition, we computed the representational similarity between two test odours in an ROI as the Pearson correlation across voxels within that region. For the posterior piriform cortex, we also quantified the relative representational proximity of Comp.CP to its two separate substructures as the difference between its correlation strengths to C_0 and P_0 in terms of voxel-wise activity patterns. The Fisher Z-transformed correlation coefficients were then compared between adaptation conditions using the paired-samples t-test.

Reporting summary
Further information on research design is available in the Nature Portfolio Reporting Summary linked to this article.

Data availability
All reported data are available at https://doi.org/10.57760/sciencedb.13818. Source data are provided with this paper.

Code availability
All analysis scripts are available at https://doi.org/10.57760/sciencedb.13818.

References

1. Mozell, M. M. & Jagodowicz, M. Chromatographic separation of odorants by the nose: retention times measured across in vivo olfactory mucosa. *Science* **181**, 1247–1249 (1973).
2. Malnic, B., Godfrey, P. A. & Buck, L. B. The human olfactory receptor gene family. *Proc. Natl Acad. Sci. USA* **101**, 2584–2589 (2004).
3. Amoore, J. E. Stereochemical theory of olfaction. *Nature* **198**, 271–272 (1963).
4. Malnic, B., Hirono, J., Sato, T. & Buck, L. B. Combinatorial receptor codes for odors. *Cell* **96**, 713–723 (1999).
5. Del Marmol, J., Yedlin, M. A. & Ruta, V. The structural basis of odorant recognition in insect olfactory receptors. *Nature* **597**, 126–131 (2021).
6. Khan, A. G., Thattai, M. & Bhalla, U. S. Odor representations in the rat olfactory bulb change smoothly with morphing stimuli. *Neuron* **57**, 571–585 (2008).
7. Soucy, E. R., Albeanu, D. F., Fantana, A. L., Murthy, V. N. & Meister, M. Precision and diversity in an odor map on the olfactory bulb. *Nat. Neurosci.* **12**, 210–220 (2009).
8. Mori, K. & Sakano, H. How is the olfactory map formed and interpreted in the mammalian brain? *Annu. Rev. Neurosci.* **34**, 467–499 (2011).
9. Ma, L. et al. Distributed representation of chemical features and tunotopic organization of glomeruli in the mouse olfactory bulb. *Proc. Natl Acad. Sci. USA* **109**, 5481–5486 (2012).
10. Barnes, D. C., Hofacer, R. D., Zaman, A. R., Rennaker, R. L. & Wilson, D. A. Olfactory perceptual stability and discrimination. *Nat. Neurosci.* **11**, 1378–1380 (2008).
11. Pashkovski, S. L. et al. Structure and flexibility in cortical representations of odour space. *Nature* **583**, 253–258 (2020).
12. Gottfried, J. A. Central mechanisms of odour object perception. *Nat. Rev. Neurosci.* **11**, 628–641 (2010).
13. Stettler, D. D. & Axel, R. Representations of odor in the piriform cortex. *Neuron* **63**, 854–864 (2009).
14. Bekkers, J. M. & Suzuki, N. Neurons and circuits for odor processing in the piriform cortex. *Trends Neurosci.* **36**, 429–438 (2013).
15. Snitz, K. et al. Predicting odor perceptual similarity from odor structure. *PLoS Comput. Biol.* **9**, e1003184 (2013).
16. Keller, A. et al. Predicting human olfactory perception from chemical features of odor molecules. *Science* **355**, 820–826 (2017).
17. Licon, C. C. et al. Chemical features mining provides new descriptive structure–odor relationships. *PLoS Comput. Biol.* **15**, e1006945 (2019).
18. Wilson, D. A. & Stevenson, R. J. The fundamental role of memory in olfactory perception. *Trends Neurosci.* **26**, 243–247 (2003).
19. Giessel, A. J. & Datta, S. R. Olfactory maps, circuits and computations. *Curr. Opin. Neurobiol.* **24**, 120–132 (2014).
20. Saha, D. et al. A spatiotemporal coding mechanism for background-invariant odor recognition. *Nat. Neurosci.* **16**, 1830–1839 (2013).
21. Nizampatnam, S., Zhang, L., Chandak, R., Li, J. & Raman, B. Invariant odor recognition with ON-OFF neural ensembles. *Proc. Natl Acad. Sci. USA* **119**, e2023340118 (2022).
22. Gottfried, J. A. Function follows form: ecological constraints on odor codes and olfactory percepts. *Curr. Opin. Neurobiol.* **19**, 422–429 (2009).
23. Frisby, J. P. *Seeing: Illusion, Brain and Mind* (Oxford Univ. Press, 1979).
24. Carhart, R. E., Smith, D. H. & Venkataraghavan, R. Atom pairs as molecular features in structure–activity studies: definition and applications. *J. Chem. Inf. Comput. Sci.* **25**, 64–73 (1985).
25. Cao, Y., Jiang, T. & Girke, T. A maximum common substructure-based algorithm for searching and predicting drug-like compounds. *Bioinformatics* **24**, i366–i374 (2008).
26. Dravnieks, A. Odor quality: semantically generated multidimensional profiles are stable. *Science* **218**, 799–801 (1982).
27. Secundo, L. et al. Individual olfactory perception reveals meaningful nonolfactory genetic information. *Proc. Natl Acad. Sci. USA* **112**, 8750–8755 (2015).
28. Nara, K., Saraiva, L. R., Ye, X. & Buck, L. B. A large-scale analysis of odor coding in the olfactory epithelium. *J. Neurosci.* **31**, 9179–9191 (2011).
29. Powell, T. P., Cowan, W. M. & Raisman, G. The central olfactory connexions. *J. Anat.* **99**, 791–813 (1965).
30. Carmichael, S. T., Clugnet, M. C. & Price, J. L. Central olfactory connections in the macaque monkey. *J. Comp. Neurol.* **346**, 403–434 (1994).
31. Lascano, A. M., Hummel, T., Lacroix, J. S., Landis, B. N. & Michel, C. M. Spatio-temporal dynamics of olfactory processing in the human brain: an event-related source imaging study. *Neuroscience* **167**, 700–708 (2010).

32. Iannilli, E., Wiens, S., Arshamian, A. & Seo, H. S. A spatiotemporal comparison between olfactory and trigeminal event-related potentials. *NeuroImage* **77**, 254–261 (2013).

33. Gottfried, J. A., Winston, J. S. & Dolan, R. J. Dissociable codes of odor quality and odorant structure in human piriform cortex. *Neuron* **49**, 467–479 (2006).

34. Li, W., Howard, J. D., Parrish, T. B. & Gottfried, J. A. Aversive learning enhances perceptual and cortical discrimination of indiscriminable odor cues. *Science* **319**, 1842–1845 (2008).

35. Howard, J. D., Plailly, J., Grueschow, M., Haynes, J. D. & Gottfried, J. A. Odor quality coding and categorization in human posterior piriform cortex. *Nat. Neurosci.* **12**, 932–938 (2009).

36. Sosulski, D. L., Bloom, M. L., Cutforth, T., Axel, R. & Datta, S. R. Distinct representations of olfactory information in different cortical centres. *Nature* **472**, 213–216 (2011).

37. Kadohisa, M. & Wilson, D. A. Separate encoding of identity and similarity of complex familiar odors in piriform cortex. *Proc. Natl Acad. Sci. USA* **103**, 15206–15211 (2006).

38. Zelano, C., Mohanty, A. & Gottfried, J. A. Olfactory predictive codes and stimulus templates in piriform cortex. *Neuron* **72**, 178–187 (2011).

39. Kriegeskorte, N. & Kievit, R. A. Representational geometry: integrating cognition, computation, and the brain. *Trends Cogn. Sci.* **17**, 401–412 (2013).

40. Turin, L. A spectroscopic mechanism for primary olfactory reception. *Chem. Senses* **21**, 773–791 (1996).

41. Rubin, B. D. & Katz, L. C. Spatial coding of enantiomers in the rat olfactory bulb. *Nat. Neurosci.* **4**, 355–356 (2001).

42. Chastrette, M. in *Olfaction, Taste, and Cognition* (eds Rouby, C. et al.) 100–116 (Cambridge Univ. Press, 2002).

43. Skaggs, E. B. Atomism versus Gestaltism in perception. *Psychol. Rev.* **47**, 347–354 (1940).

44. Moncrieff, R. W. Olfactory adaptation and odour likeness. *J. Physiol.* **133**, 301–316 (1956).

45. Cain, W. S. Odor intensity after self-adaptation and cross-adaptation. *Percept. Psychophys.* **7**, 271–275 (1970).

46. Cain, W. S. & Polak, E. H. Olfactory adaptation as an aspect of odor similarity. *Chem. Senses* **17**, 481–491 (1992).

47. Pierce, J. D. Jr, Zeng, X. N., Aronov, E. V., Preti, G. & Wysocki, C. J. Cross-adaptation of sweaty-smelling 3-methyl-2-hexenoic acid by a structurally-similar, pleasant-smelling odorant. *Chem. Senses* **20**, 401–411 (1995).

48. Pierce, J. D. Jr, Wysocki, C. J., Aronov, E. V., Webb, J. B. & Boden, R. M. The role of perceptual and structural similarity in cross-adaptation. *Chem. Senses* **21**, 223–237 (1996).

49. Gori, M., Giuliana, L., Sandini, G. & Burr, D. Visual size perception and haptic calibration during development. *Dev. Sci.* **15**, 854–862 (2012).

50. Thompson, R. in *International Encyclopedia of the Social and Behavioral Sciences* (eds Smelser, N. J. & Baltes, P. B.) 6458–6462 (Pergamon, 2001).

51. Pellegrino, R., Sinding, C., de Wijk, R. A. & Hummel, T. Habituation and adaptation to odors in humans. *Physiol. Behav.* **177**, 13–19 (2017).

52. Li, W., Luxenberg, E., Parrish, T. & Gottfried, J. A. Learning to smell the roses: experience-dependent neural plasticity in human piriform and orbitofrontal cortices. *Neuron* **52**, 1097–1108 (2006).

53. Mori, K., Takahashi, Y. K., Igarashi, K. M. & Yamaguchi, M. Maps of odorant molecular features in the mammalian olfactory bulb. *Physiol. Rev.* **86**, 409–433 (2006).

54. Fournel, A., Ferdenzi, C., Sezille, C., Rouby, C. & Bensafi, M. Multidimensional representation of odors in the human olfactory cortex. *Hum. Brain Mapp.* **37**, 2161–2172 (2016).

55. Chu, M. W., Li, W. L. & Komiyama, T. Balancing the robustness and efficiency of odor representations during learning. *Neuron* **92**, 174–186 (2016).

56. Kass, M. D., Guang, S. A., Moberly, A. H. & McGann, J. P. Changes in olfactory sensory neuron physiology and olfactory perceptual learning after odorant exposure in adult mice. *Chem. Senses* **41**, 123–133 (2016).

57. Tsukahara, T. et al. A transcriptional rheostat couples past activity to future sensory responses. *Cell* **184**, 6326–6343 e6332 (2021).

58. Farkhooi, F., Froese, A., Muller, E., Menzel, R. & Nawrot, M. P. Cellular adaptation facilitates sparse and reliable coding in sensory pathways. *PLoS Comput. Biol.* **9**, e1003251 (2013).

59. Patterson, C. A., Wissig, S. C. & Kohn, A. Adaptation disrupts motion integration in the primate dorsal stream. *Neuron* **81**, 674–686 (2014).

60. Verhagen, J. V., Wesson, D. W., Netoff, T. I., White, J. A. & Wachowiak, M. Sniffing controls an adaptive filter of sensory input to the olfactory bulb. *Nat. Neurosci.* **10**, 631–639 (2007).

61. Kermen, F. et al. Molecular complexity determines the number of olfactory notes and the pleasantness of smells. *Sci. Rep.* **1**, 206 (2011).

62. Roblin, D. G. & Eccles, R. Normal range for nasal partitioning of airflow determined by nasal spirometry in 100 healthy subjects. *Am. J. Rhinol.* **17**, 179–183 (2003).

63. Mai, J. K., Paxinos, G. & Voss, T. *Atlas of the Human Brain* 3rd edn (Academic Press, 2008).

64. Eickhoff, S. B. et al. A new SPM toolbox for combining probabilistic cytoarchitectonic maps and functional imaging data. *NeuroImage* **25**, 1325–1335 (2005).

65. Gottfried, J. A. & Zald, D. H. On the scent of human olfactory orbitofrontal cortex: meta-analysis and comparison to non-human primates. *Brain Res. Brain Res. Rev.* **50**, 287–304 (2005).

Acknowledgements

Author contributions

W.Z. conceptualized the study. Y.Y., Y.W., Y.Z., H.T., H.Y. and K.Y. performed the experiments. Z.Z. optimized the imaging parameters. Y.Y., Y.W. and H.T. analysed the data under the supervision of W.Z. Y.Y., Y.W. and W.Z. wrote the manuscript.

Competing interests

The authors declare no competing interests.

Additional information

Supplementary information The online version contains supplementary material available at https://doi.org/10.1038/s41562-024-01849-0.

Correspondence and requests for materials should be addressed to Wen Zhou.

Peer review information *Nature Human Behaviour* thanks Emilia Iannilli, Wen Li and the other, anonymous, reviewer(s) for their contribution to the peer review of this work. Peer reviewer reports are available.

Reprints and permissions information is available at www.nature.com/reprints.

Corresponding author(s): Wen Zhou

Last updated by author(s): Feb 8, 2024

Reporting Summary

Nature Portfolio wishes to improve the reproducibility of the work that we publish. This form provides structure for consistency and transparency in reporting. For further information on Nature Portfolio policies, see our Editorial Policies and the Editorial Policy Checklist.

Statistics

For all statistical analyses, confirm that the following items are present in the figure legend, table legend, main text, or Methods section.

n/a	Confirmed	
☐	☒	The exact sample size (*n*) for each experimental group/condition, given as a discrete number and unit of measurement
☐	☒	A statement on whether measurements were taken from distinct samples or whether the same sample was measured repeatedly
☐	☒	The statistical test(s) used AND whether they are one- or two-sided *Only common tests should be described solely by name; describe more complex techniques in the Methods section.*
☐	☒	A description of all covariates tested
☐	☒	A description of any assumptions or corrections, such as tests of normality and adjustment for multiple comparisons
☐	☒	A full description of the statistical parameters including central tendency (e.g. means) or other basic estimates (e.g. regression coefficient) AND variation (e.g. standard deviation) or associated estimates of uncertainty (e.g. confidence intervals)
☐	☒	For null hypothesis testing, the test statistic (e.g. F, t, r) with confidence intervals, effect sizes, degrees of freedom and P value noted *Give P values as exact values whenever suitable.*
☒	☐	For Bayesian analysis, information on the choice of priors and Markov chain Monte Carlo settings
☒	☐	For hierarchical and complex designs, identification of the appropriate level for tests and full reporting of outcomes
☐	☒	Estimates of effect sizes (e.g. Cohen's *d*, Pearson's *r*), indicating how they were calculated

Our web collection on statistics for biologists contains articles on many of the points above.

Software and code

Policy information about availability of computer code

Data collection	No software was used for data collection in the behavioral assessments. E-prime 2.0 was used to control odor deliveries, present visual prompts and record responses in the fMRI experiment.
Data analysis	SPSS (Version 26), JASP (Version 0.13), Matlab 2014a, SPM 12, and AFNI 20.2.08.

For manuscripts utilizing custom algorithms or software that are central to the research but not yet described in published literature, software must be made available to editors and reviewers. We strongly encourage code deposition in a community repository (e.g. GitHub). See the Nature Portfolio guidelines for submitting code & software for further information.

Data

Policy information about availability of data

All manuscripts must include a data availability statement. This statement should provide the following information, where applicable:

- Accession codes, unique identifiers, or web links for publicly available datasets
- A description of any restrictions on data availability
- For clinical datasets or third party data, please ensure that the statement adheres to our policy

All presented data and analysis scripts are available at https://doi.org/10.57760/sciencedb.13818.

Human research participants

Reporting on sex and gender	The study examines the perception and neural representation of odor molecules. Sex and gender were not considered in the study design. Participants self-reported their sex. 51.6% of those who took part in the behavioral assessments and 50% of those in the fMRI experiment were female. No sex- and gender-based analyses have been performed as the study is not designed to probe sex- or gender-related differences.
Population characteristics	See above.
Recruitment	Participants were recruited via advertisement on social media.
Ethics oversight	The study was approved by the Institutional Review Board at the Institute of Psychology, Chinese Academy of Sciences (H18029).

Note that full information on the approval of the study protocol must also be provided in the manuscript.

Field-specific reporting

Please select the one below that is the best fit for your research. If you are not sure, read the appropriate sections before making your selection.

☐ Life sciences   ☒ Behavioural & social sciences   ☐ Ecological, evolutionary & environmental sciences

For a reference copy of the document with all sections, see nature.com/documents/nr-reporting-summary-flat.pdf

Behavioural & social sciences study design

All studies must disclose on these points even when the disclosure is negative.

Study description	The study presents quantitative data from nine behavioral experiments and an fMRI experiment where olfactory perception and neural representations of monomolecular odorants were compared before and after substructure adaptation, superstructure adaptation, and/or nonspecific olfactory adaptation.
Research sample	A total of 458 healthy non-smokers (236 female, mean age: 23.1 yrs, SD: 1.8 yrs) with no history of neurological disorders participated in the study. Of these, 386 participated in the main study and 36 in each of Supplementary Experiments 1 and 2. For the main study, 360 participants took part in the various behavioral assessments (36 participants per condition or task) and 26 participated in the fMRI experiment. They reported to have a normal sense of smell and no respiratory allergy or upper respiratory infection at the time of testing. Those who took part in unilateral adaptation and test also had no significant nasal septal deviation as measured by nasal spirometry, with nasal partitioning ratios ranging between −0.3 and 0.3.
Sampling strategy	Participants were selected based on the following criteria: 18-30 years old, nonsmoker, a normal sense of smell, no respiratory allergy or upper respiratory infection at the time of testing, no history of neurological disorders. In addition, for the unilateral adaptation and test experiment: no significant nasal septal deviation as determined by nasal spirometry; for the fMRI experiment: fulfillment of the MR safety criteria (e.g., no metal implant, no claustrophobia, etc). As to sample sizes, we were unaware of any previous study on substructure adaptation and odor quality change and thus could not perform a formal power analysis. The sample size in each experiment (or cell) was about twice the size used in previous studies on related topics (Cain & Polak, 1992; Gottfried et al., 2006; Howard et al., 2009; Li et al., 2008; Pierce et al., 1996; Pierce et al., 1995; Zelano et al., 2011).
Data collection	For the behavioral assessments, participants were individually assessed by an experimenter in a well-ventilated room (see Behavioral assessments for details). No one else was present during testing. The data were recorded by pen and paper. For the fMRI experiment, MR images were collected using Siemens Prisma 3T scanner; responses in the scanner were recorded using a keypad attached to the participants' right hand. No one was present in the scan room with the participants during scanning. Both the participants and the experimenters were blind to the chemical relationships among the olfactory stimuli and to the specific purposes of the experiments during data collection.
Timing	Data collection for the main study started in March 2019 and ended in August 2021. Supplementary experiments were performed from February to May 2023.
Data exclusions	No data were excluded from the analyses.
Non-participation	Five participants dropped out of the 2-session behavioral experiments due to time conflicts.
Randomization	Participants were randomly allocated into different experimental groups where applicable.

Reporting for specific materials, systems and methods

We require information from authors about some types of materials, experimental systems and methods used in many studies. Here, indicate whether each material, system or method listed is relevant to your study. If you are not sure if a list item applies to your research, read the appropriate section before selecting a response.

Materials & experimental systems

n/a	Involved in the study
☒	☐ Antibodies
☒	☐ Eukaryotic cell lines
☒	☐ Palaeontology and archaeology
☒	☐ Animals and other organisms
☒	☐ Clinical data
☒	☐ Dual use research of concern

Methods

n/a	Involved in the study
☒	☐ ChIP-seq
☒	☐ Flow cytometry
☐	☒ MRI-based neuroimaging

Magnetic resonance imaging

Experimental design

Design type

Slow event-related fMRI design.

Design specifications

The fMRI experiment comprised two scanning sessions held on two separate days, with Comp.CP as the adapting odor in one session and P in the other session. Each session consisted of 6 runs of about 6 min each: 2 baseline runs without adaptation, followed by 4 adaptation runs where the adapting odor of that session was delivered (in place of purified air) before the start of the first trial and during all inter-trial intervals. Each trial began with a 2 s attentional prompt, after which participants were cued to take a 2 s sniff. They then indicated with a button press whether there was an odor (for baseline runs) or whether there was an odor different from the background odor (for adaptation runs). There were 14 trials per baseline run: Comp.CP, P, C, and purified air were each presented during the sniff cue in 4, 4, 4, and 2 trials, respectively, in a pseudo-randomized order, and the interstimulus interval was jittered between 18 to 30 s. There were 13 trials per adaptation run: Comp.CP, P, and C were each presented in 3, 5, and 5 trials, respectively, when Comp.CP was the adapting odor, and in 5, 3, and 5 trials, respectively, when P was the adapting odor. The interstimulus interval was jittered between 18 to 26 s.

Behavioral performance measures

Participants' button presses (Y/N) were recorded. Task performance was assessed with hit rate. Hit rates in the baseline runs and adaptation runs were respectively calculated and compared.

Acquisition

Imaging type(s)

Functional and structural MRI.

Field strength

3 Tesla.

Sequence & imaging parameters

Gradient-echo T2*-weighted echoplanar images (EPI) were acquired with two sets of parameters due to a major software update. For 17 participants: repetition time (TR), 2 s; echo time, 27 ms; flip angle, 90°; matrix, 96 × 96; field of view, 192 × 192 mm2; in-plane resolution, 2.0 × 2.0 mm2; slice thickness, 2 mm; gap, 0; number of slices, 34; and acquisition angle, 30° rostral to the intercommissural line. For 9 participants: a blipped-controlled-aliasing multiband EPI sequence was employed; TR, 2 s; echo time, 29 ms; flip angle, 80°; matrix, 128 × 128; field of view, 192 × 192 mm2; in-plane resolution, 1.5 × 1.5 mm2; slice thickness, 1.5 mm; gap, 0; number of slices, 88; and acquisition angle, 0° to the intercommissural line. A 1 mm3 isotropic T1-weighted anatomical volume, along with a field map, was also acquired for each participant.

Area of acquisition

For 17 participants, 34 slices were acquired at an oblique plane 30° rostral to the intercommissural line, which covered all regions of interest including the anterior piriform cortex, posterior piriform cortex, amygdala, and orbitofrontal cortex.
For 9 participants, a whole-brain scan was acquired.

Diffusion MRI ☐ Used ☒ Not used

Preprocessing

Preprocessing software

SPM 12 (http://www.fil.ion.ucl.ac.uk/spm). Preprocessing involved slice timing correction, artifact removal, motion correction, and for univariate analysis, spatial smoothing (6-mm FWHM Gaussian kernel) and temporal filtering (128 s high-pass filter). For representational similarity analysis, no additional preprocessing was performed to preserve the spatial fidelity of the signals.

Normalization

Spatial normalization was not performed except for the purpose of displaying group-level odor-induced activations at

Normalization	baseline, in which case the images from the baseline runs were spatially normalized to a standard EPI template (MNI space).
Normalization template	ICBM152.
Noise and artifact removal	EPI images were corrected for geometric distortion due to susceptibility artifacts using participants' field maps and were spatially realigned to the first volume of the first session (first baseline run on Day 1) and unwarped to reduce movement related variance. In the GLM-based univariate analysis, movement parameters were entered as nuisance regressors.
Volume censoring	Not applied.

Statistical modeling & inference

Model type and settings	We performed both univariate analysis and multivariate representational similarity analysis. For univariate analysis, the 3 × 3 combinations of test odors (Comp.CP, P, C) and adaptation conditions (baseline, adaptation to Comp.CP, adaptation to P) were modeled with a set of impulse response functions from 0-16 s post stimulus that made no assumption about the shape of the response. Head motion parameters were included as nuisance regressors, and serial autocorrelations were modeled as an autoregressive process. For multivariate representational similarity analysis, we computed and compared the representational similarities between two test odors in an ROI under different adaptation conditions.
Effect(s) tested	We tested the effect of adaptation condition on odor-evoked percent signal changes in the ROIs with repeated measures ANOVAs and paired-sample t tests. In addition, the representational similarities (z-transformed Pearson correlations) between two test odors in each ROI were compared between adaptation conditions using the paired-samples t test.

Specify type of analysis: ☐ Whole brain ☒ ROI-based ☐ Both

Anatomical location(s)	The anterior piriform cortex and the posterior piriform cortex were manually drawn on each participant's anatomical scan, coregistered to his/her mean realigned EPI image, according to an anatomical atlas (Mai et al., 2008). The amygdala was defined using cytoarchitectonic probabilistic maps integrated in SPM Anatomy toolbox (Eickhoff et al., 2005). The olfactory orbitofrontal cortex was defined based on a meta-analysis of human neuroimaging studies on olfactory processing (Gottfried and Zald, 2005), drawn as 6-mm radius spheres centered on MNI coordinates (-22, 32, -18) and (24, 33, -12), respectively.
Statistic type for inference (See Eklund et al. 2016)	The structural masks of the ROIs were projected into each participant's native EPI space and functionally restricted to voxels that responded to odors at baseline (voxel-wise $p < 0.01$) (Zelano et al, 2011). The functionally restricted ROIs were employed in all subsequent analysis. Statistical inferences were based on odor-evoked percent signal changes and the representational similarities between two test odors extracted from the ROIs under different adaptation conditions.
Correction	Multiple comparisons across ROIs and conditions were Bonferroni corrected where applicable.

Models & analysis

n/a	Involved in the study
☒ ☐	Functional and/or effective connectivity
☒ ☐	Graph analysis
☐ ☒	Multivariate modeling or predictive analysis

Multivariate modeling and predictive analysis	For multivariate representational similarity analysis, effects of no interest (motion regressors and low-frequency drift) were first subtracted out from the preprocessed functional data with AFNI programs 3dDeconvolve and 3dSynthesize. Values from post-stimulus TR 3, the time point that best captured signal variations across conditions, were then extracted from the voxels within each ROI for each of the combinations of test odors and adaptation conditions, which formed the input to representational similarity analysis. For each adaptation condition, we computed the representational similarity between two test odors in an ROI as the Pearson correlation across voxels within that region.

nature portfolio | reporting summary

March 2021

4